ChemPubSoc Europe

DOI: 10.1002/chem.201805679

CHEMISTRY
A European Journal
Communication

Molecular Evolution |Hot Paper|

Increase of Redox Potential during the Evolution of Enzymes Degrading Recalcitrant Lignin

Iván Ayuso-Fernández,[a] Antonio L. De Lacey,[b] Francisco J. Cañada,[a] Francisco J. Ruiz-Dueñas,[a] and Angel T. Martínez*[a]

Abstract: To investigate how ligninolytic peroxidases acquired the uniquely high redox potential they show today, their ancestors were resurrected and characterized. Unfortunately, the transient Compounds I (CI) and II (CII) from peroxide activation of the enzyme resting state (RS) are unstable. Therefore, the reduction potentials ($E^{\circ\prime}$) of the three redox couples (CI/RS, CI/CII and CII/RS) were estimated (for the first time in a ligninolytic peroxidase) from equilibrium concentrations analyzed by stopped-flow UV/Vis spectroscopy. Interestingly, the $E^{\circ\prime}$ of rate-limiting CII reduction to RS increased 70 mV from the common peroxidase ancestor to extant lignin peroxidase (LiP), and the same boost was observed for CI/RS and CI/CII, albeit with higher $E^{\circ\prime}$ values. A straightforward correlation was found between the $E^{\circ\prime}$ value and the progressive displacement of the proximal histidine Hε1 chemical shift in the NMR spectra, due to the higher paramagnetic effect of the heme Fe^{3+}. More interestingly, the $E^{\circ\prime}$ and NMR data also correlated with the evolutionary time, revealing that ancestral peroxidases increased their reduction potential in the evolution to LiP thanks to molecular rearrangements in their heme pocket during the last 400 million years.

The use of paleogenetics to investigate protein properties in evolution is a developing field that has been used to prove different evolutionary hypotheses.[1] Using a robust phylogeny and the ancestral sequence reconstruction tools, the time travel investigation of any family of proteins is virtually possible, even to the early stages of earth.[2] Lignin peroxidases (LiP), versatile peroxidases (VP) and manganese peroxidases (MnP)[3] belong to the peroxidase-catalase superfamily.[4] These fungal heme proteins are characterized by a high reduction potential enabling oxidation of the recalcitrant (non-phenolic) lignin polymer formed by the dehydrogenative polymerization of phenolic monolignols by low redox potential plant peroxidases.[5] Lignin biodegradation, which was defined as an enzymatic combustion,[6] is a key step for carbon recycling in land ecosystems and a process of biotechnological interest for the use of plant biomass in a bio-based economy.[7,8]

The evolutionary changes in ligninolytic peroxidases have been recently investigated[9,10] by resurrection of ancestral enzymes from sequenced genomes of Polyporales,[11] in which most lignin-degrading fungi are included. In this way, the transition from an ancestor that oxidized lignin poorly using diffusible Mn^{3+} chelates, around 400 million years ago,[12] into more efficient enzymes that oxidized lignin directly was demonstrated.[9] That powerful degradative strategy was acquired when a solvent-exposed tryptophanyl radical appeared in an ancestral VP, and became more efficient in ancestral and extant LiPs. The latter include LiP-H8 from the model fungus *Phanerochaete chrysosporium*,[13] corresponding to LiPA (PC-LiPA) in the sequenced genome,[14] the molecular structure of which is shown in Figure 1. Direct degradation of lignin emerged independent-

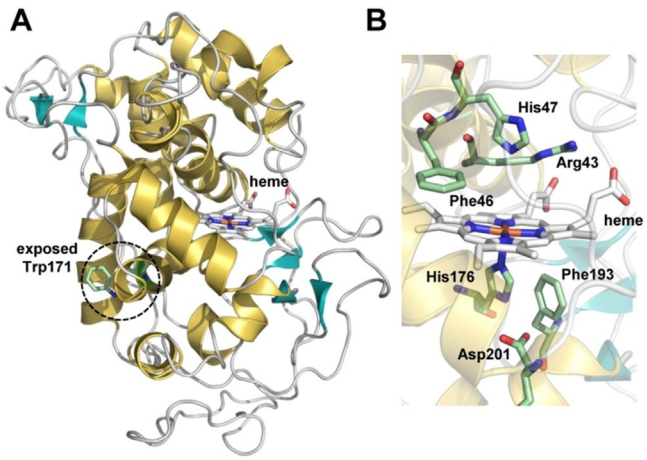

Figure 1. General model of *P. chrysosporium* LiP showing the secondary structure of the protein, the buried heme cofactor and the catalytic tryptophan exposed to the solvent (A), and detail of the heme pocket with two axial histidines and other residues (B). From PDB 1LGA.

[a] I. Ayuso-Fernández, Prof. Dr. F. J. Cañada, Dr. F. J. Ruiz-Dueñas, Prof. Dr. A. T. Martínez
Centro de Investigaciones Biológicas, CSIC
Ramiro de Maeztu 9, E-28040, Madrid (Spain)
E-mail: atmartinez@cib.csic.es

[b] Dr. A. L. De Lacey
Instituto de Catálisis y Petroleoquímica, CSIC
Marie Curie 2, E-28049 Madrid (Spain)

Supporting information and the ORCID identification number(s) for the author(s) of this article can be found under: https://doi.org/10.1002/chem.201805679.

ly several times in peroxidase evolution,[10] showing the importance of lignin decay (by fungi) during land colonization by vascular plants.[12] To elucidate if ligninolytic peroxidases 1) acquired their oxidizing power with evolution or 2) they were already high redox potential enzymes in ancestral Polyporales peroxidases and later shaped their oxidation sites, we analyzed the evolutionary lineage leading to PC-LiPA (Figure S1, Supporting Information) by ancestral sequence reconstruction from the genomes of ten Polyporales species[11] using the PAML software.[15] The most relevant ancestral sequences in the PC-LiPA lineage were "resurrected", corresponding to: 1) common ancestor of Polyporales peroxidases (CaPo); 2) common ancestor of clade D peroxidases (CaD); 3) first ancestral VP in clade D (AVPd); and 4) first ancestral LiP (ALiP) (multiple alignment in Figure S2, Supporting Information). The four ancestral peroxidases and the extant LiPA were characterized, including the reduction potential estimation for the different redox pairs in the catalytic cycle.

To understand the evolution of the peroxidase redox properties, the three steps of their catalytic cycle[16] were analyzed (Figure 2). The initial reaction is the oxidation of the resting state (RS) enzyme by H_2O_2, extracting two electrons from the cofactor. This generates Compound I (CI) with two oxidizing equivalents (as $Fe^{4+}=O$ and porphyrin cation radical complex). Alternatively, CI of LiP/VP transfers one of these equivalents forming the above mentioned solvent-exposed tryptophanyl radical directly oxidizing the bulky lignin polymer,[17,18] which is unable to access the buried cofactor.[19] CI is reduced to Compound II (CII) during oxidation of a substrate molecule. CII has one oxidation equivalent ($Fe^{4+}=O$, in equilibrium with the tryptophanyl radical in LiP/VP), and is further reduced to the RS by oxidation of another molecule of substrate.

The most common redox measurement in heme proteins, basidiomycete peroxidases included,[20–25] is the midpoint potential of the ferric/ferrous transition (Figures S3 and S4, Supporting Information), even though it is not part of the catalytic cycle (Figure 2). To explore the mechanistic implications of reduction potential in the peroxidase catalytic cycle, we used stopped-flow spectrophotometry[26–29] to measure the concentration of the oxidized and reduced forms of the different enzymes in their RS/CI and CII/RS transitions (Figures S5 and S6, respectively) as illustrated in Figure 3 for the most recent ancestor. Stopped flow was used here to assign the equilibrium concentrations of the two redox states of the enzyme and the two redox states of the substrates used, providing an equilibrium constant that, with the use of the Nerst equation, will allow for the determination of the midpoint potential. In this way, the reduction potentials of the catalytic iron couples (those of CI/RS and CII/RS directly, and the CI/CII $E^{\circ\prime}$ by difference) were calculated for the first time in ligninolytic peroxidases (see Supporting Information, section Supplementary Methods and Tables for details). Analysis of the three half-reactions revealed a general boost of the reduction potentials with evolution (Figure 4). For all the redox pairs (CI/RS, CI/CII and CII/RS) we obtained differences of approximately 70 mV between the oldest ancestor (CaPo) and ALiP, which had the highest reduction potentials (close to the values of extant PC-LiPA).

Starting with the activation by H_2O_2, the $E^{\circ\prime}$(CI/RS) values increase progressively from CaPo (1.34 V) to ALiP (1.41 V), being that value stabilized in extant LiP (Figure 4, center). Although the increasing difficulty to oxidize the enzyme through evolu-

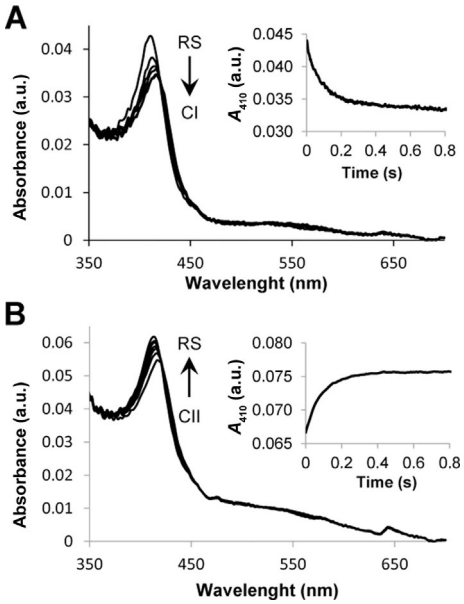

Figure 3. Redox equilibrium analysis by stopped flow. (A) Spectral changes upon rapid mixing of ALiP RS with H_2O_2 to follow CI formation (from 1.6 to 800 ms after peroxide addition). (B) Spectral changes during tyrosine reduction of CII, formed by enzyme mixing with H_2O_2 and ferrocyanide (from 1.6 to 800 ms after tyrosine addition). The insets show time traces at 410 nm (near Soret maximum) to attain equilibrium conditions. All reactions were at the optimal pH 3, and at 25 °C.

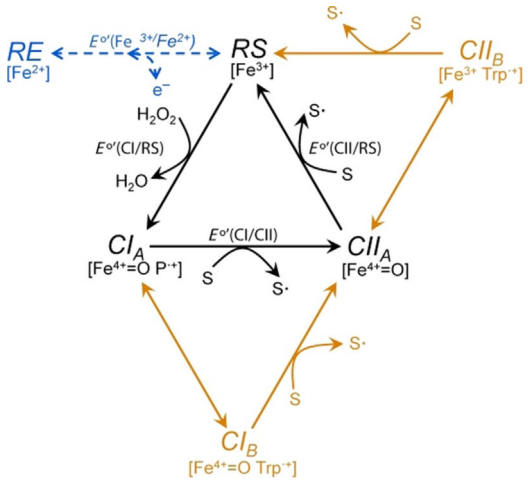

Figure 2. Ligninolytic peroxidase catalytic cycle. Black: the common cycle initiated with oxidation of the RS enzyme by peroxide, followed by two substrate (S) one-electron oxidations (by CI and CII). Orange: the expanded cycle of VPs and LiPs, with formation of a tryptophanyl radical. The blue dashed line leading to the ferrous reduced enzyme (RE-Fe^{2+}) is not part of the cycle, but it has been studied here. The formal reduction potentials ($E^{\circ\prime}$) analyzed are indicated. Adapted from Ref. [17].

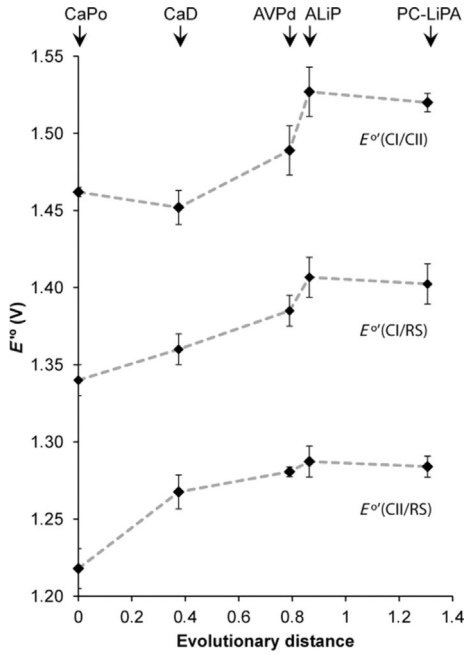

Figure 4. $E^{\circ\prime}$ values for the three redox couples in the catalytic cycle (Figure 2) versus evolutionary distance (see Ref. [10]). The $E^{\circ\prime}$(CI/RS) and $E^{\circ\prime}$(CII/RS) values were from stopped-flow, whereas the $E^{\circ\prime}$(CI/CII) values were from equation $\Delta G_r^{\circ\prime} = -n{\cdot}F{\cdot}E^{\circ\prime}$ (see the Supporting Information).

tion seems a disadvantage, the reduction potential of this two-electron oxidation is connected to the subsequent one-electron oxidations of substrates[29] [Equation (8) in the Supporting Information, Supplementary Materials and Methods]; the free energy of the activation reaction being the sum of the free energies of the two one-electron oxidations of substrate. Therefore, the higher the $E^{\circ\prime}$(CI/RS), the higher will be the free energy in the subsequent steps, being the oxidation of high redox potential substrates favored in evolution.

The two one-electron oxidations showed strong differences between the $E^{\circ\prime}$(CI/CII) and $E^{\circ\prime}$(CII/RS) values (Figure 4, top and bottom, respectively). Variations of about 0,2 V were observed in all cases, with the $E^{\circ\prime}$(CI/CII) values being the highest, as reported for other peroxidases.[27,29,30] As a result for this high reduction potential, it is expected for CI to be rapidly reduced to CII in the presence of the electron-donor ferrocyanide, as observed in every enzyme analyzed. Moreover, it has been estimated from quantum mechanics/molecular mechanics calculations that, at low pH, the reduction potential would increase due to protonation of negative charges that stabilize CI,[31] with an estimation of $E^{\circ\prime} > 1.2$ V for the PC-LiPA CI/CII couple at pH 3.[32] Here, we estimated for the first time this reduction potential of PC-LiPA at pH 3, the ecophysiological pH of lignin biodegradation in nature,[33] with a value (1.52 V) that widely exceeds those estimations. More importantly, the $E^{\circ\prime}$(CII/RS) also improved in evolution, and the potentials obtained for extant and ancestral peroxidases are the lowest in the catalytic cycle, explaining why this half-reaction is the limiting step in the oxidation of lignin.[17]

The reduction potentials of the three redox couples in extant/ancestral fungal ligninolytic peroxidases are higher than those reported for most animal,[27] plant[34] or prokaryotic[30] peroxidases, usually estimated at pH 7. However, the differences with the $E^{\circ\prime}$ (CI/RS) values of some animal peroxidases,[27] which were estimated with a similar stopped-flow method, would be small after considering the variation (around 0.2 V) existing between the pH 7 and pH 3 estimations,[22,35,36] due to the presence of one or several protonable residues contributing to peroxidase catalysis.[25,37] The values shown here are also slightly higher than the $E^{\circ\prime}$ of 1.3 V estimated at pH 3, with the stopped-flow method, for the CI/RS couple of fungal chloroperoxidase and peroxygenase,[36] two heme-thiolate proteins related to cytochrome P450 monooxygenases.

Additionally, some clues on the structural changes that led to the above boost of reduction potential in the PC-LiPA lineage were provided by ^{1}H NMR spectra of the cyanide adducts of the extant and ancestral enzymes (Figure 5 A), in which the

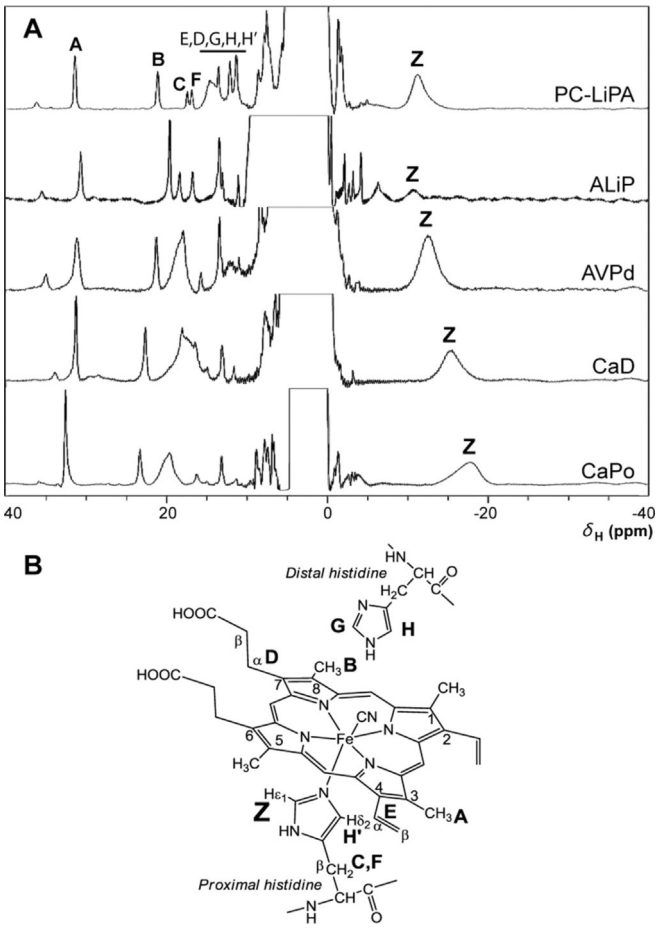

Figure 5. (A) ^{1}H NMR spectra of CN adducts of the ancestral and extant enzymes. Some signals were assigned by comparison with the literature. By homology, in all enzymes the signal Z with the largest high field shift was assigned to the Hε1 of the proximal histidine directly coordinated to the heme Fe^{3+}, whereas the other low-field shifted labeled signals (>10 ppm), correspond to the heme $3CH_3$ (A), $8CH_3$ (B), 7α (D) and 4α (E), the proximal histidine Hβ (C), Hβ′ (F) and Hδ2 (H′) and the distal histidine Hε1(G) and Hδ2(H). Spectra (in 50 mM phosphate, pH 6.5, prepared with ^2H_2O) were acquired with high scanning rate using water eliminated Fourier transform (WEFT) pulse sequence (Ref. [47]) with a short delay to maximize fast relaxing signals. (B) Representation of heme–CN complex as well as proximal and distal histidines, with numbering and labels, as in Ref. [38] by Banci et al..

cyanide carbon occupies the position of oxygen in CI/CII, acquired at pH 6.5 to promote enzyme stability and solubility. Analyses under similar conditions have shown that the strength of the bond between the proximal histidine (His176) and the heme Fe^{3+}, and the geometry of the complex (Figure 5B), would influence the redox properties of heme peroxidases, from ancient peroxidases of prokaryotic origin to the more recent peroxidases of basidiomycetes,[38–42] by controlling the imidazolate character of the histidine and the electron deficiency of the iron. The above correlates with the characteristic hyperfine chemical shifts of imidazole protons. These strong hyperfine shifts, induced by the iron paramagnetism, have been extensively used to assign the ^{1}H NMR signals on the amino acids surrounding the heme group in the peroxidases.[43,44] Interestingly, the ring protons of proximal histidine appear as very broad signals, being the Hε1 isolated and located in the upfield area, whereas the Hδ2 is located in the more crowded downfield area.[45,46]

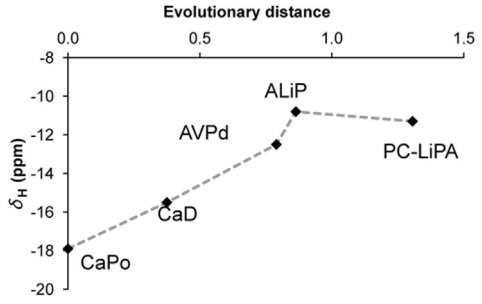

Figure 6. Representation of the evolutionary distance of the ancestral and extant enzymes (Ref. [10]) using the chemical shift (δ_H) of signal Z in the ^{1}H NMR spectra of their CN adducts, which is shown in Figure 5.

Here, we show a significant change in evolution of the Hε1 chemical shift of the proximal histidine (Figure 6), and the same trend was found at pH 3 (not shown) despite the lower peroxidase stability than that at pH 6.5. The gradual δ_H displacement from CaPo (−18 ppm) to ALiP/PC-LiPA (−11 ppm) correlates with a reduction of the imidazolate character of the proximal histidine[40] (due to changes in side-chain distance and/or orientation caused by variable heme/histidine environments) indicative of a weaker axial bond between the histidine side chain and the heme Fe^{3+}, which, in turns, destabilizes the higher oxidation state of the heme iron.[38] Interestingly, this change correlates with the changes observed in the reduction potentials: progressively higher $E^{\circ\prime}$ for the three steps in the peroxidase cycle. This is uniquely interesting, considering that it is the first time that structural data from NMR are correlated with reduction potential measurements of the catalytic cycle couples. Moreover, NMR and stopped-flow changes correlate also with evolutionary time from the common ancestor of Polyporales peroxidases about 400 million years ago.[12] This leads to the main conclusion that, during this period, ligninolytic peroxidases increased their already high redox potential by molecular rearrangement in the proximal side of the heme pocket.

The general boost of reduction potentials sums to other adaptations reported in ligninolytic peroxidase evolution. It has been demonstrated that these enzymes became more stable at acidic pH, at which they act in nature,[33] when they acquired the solvent-exposed tryptophan that oxidize lignin directly.[9] The environment surrounding this tryptophan was also shaped in evolution increasing the oxidation power of the tryptophanyl radical and stabilizing the substrate radical cation intermediates. In particular, the more than five-fold higher efficiency of PC-LiPA oxidizing the simple lignin model compound veratryl alcohol can be connected with the above environment, which is more negative than in its ancestors.[10] Therefore, it seems that, once a high enough reduction potential had been attained (in ALiP), the peroxidase final evolutionary step focused on increasing the acidic stability and selecting a more acidic tryptophanyl radical environment in extant LiP. As a whole, ancestral enzyme resurrection illustrates how LiPs became the most efficient enzymes degrading lignin.

The present study provides new information on the uniquely high reduction potential of enzymes of biotechnological interest due to their ability to degrade lignin, a key issue in lignocellulose biorefineries for the production of bio-based chemicals, fuels and materials.[7]

Experimental Section

Methods: The 113 sequences of class-II peroxidases[4] in the genomes of *Bjerkandera adusta*, *Ceriporiopsis subvermispora*, *Dichomitus squalens*, *Fomitopsis pinicola*, *Ganoderma sp.*, *Phlebia brevispora*, *P. chrysosporium*, *Postia placenta*, *Trametes versicolor* and *Wolfiporia cocos*,[11] available at the DOE JGI (https://genome.jgi.doe.gov/programs/fungi/index.jsf), were used in this study. After sequence alignment with MUSCLE as implemented in Mega X,[48] ML phylogeny was constructed with RAxML,[49] and PAML 4.7[15] was used to obtain the most probable ancestral sequences, which were manually corrected for insertions or deletions, and synthesized for *E. coli* expression. The coding DNA sequences of ancestral and extant peroxidases were cloned and used to transform *E. coli*, and expressed and purified as previously described.[9] $E^{\circ\prime}$ values of the catalytic cycle were calculated using stopped-flow spectrophotometry,[26–29] using tyrosine as reducing substrate, and the $E^{\circ\prime}$ (Fe^{3+}/Fe^{2+}) was obtained through spectrophotometric titration.[22]. ^{1}H NMR spectra of CN adducts of all enzymes were collected, as previously reported for other heme peroxidases,[38] to analyze the displacement with evolution of the signals corresponding to the proximal histidine. For more details see the Supporting Information.

Acknowledgements

This work has been funded by the EnzOx2 (BBI-PPP-2015-2-720297; www.enzox2.eu) EU project, and the CTQ2015-71290-R, BFU2016-77835-R and BIO2017-86559-R projects of the Spanish Ministry of Economy, Industry and Competitiveness, cofinanced by FEDER funds. The NMR service of CIB and M. Carmen Fernández are acknowledged for acquiring the NMR spectra. The authors thank Paul G. Furtmüller and Roland Ludwig (BOKU, Vienna) for advice in stopped-flow determina-

tion of reduction potentials, and Werner Mäntele (University of Frankfurt) for kindly providing the spectroelectrochemical cell.

Conflict of interest

The authors declare no conflict of interest.

Keywords: ancestral enzymes · molecular evolution · protein NMR · redox chemistry · stopped–flow equilibrium

[1] Y. Gumulya, E. M. J. Gillam, *Biochem. J.* **2017**, *474*, 1.
[2] V. A. Risso, J. A. Gavira, D. F. Mejia-Carmona, E. A. Gaucher, J. M. Sanchez-Ruiz, *J. Am. Chem. Soc.* **2013**, *135*, 2899 – 2902.
[3] F. J. Ruiz-Dueñas, M. Morales, E. García, Y. Miki, M. J. Martínez, A. T. Martínez, *J. Exp. Bot.* **2009**, *60*, 441 – 452.
[4] M. Zámocký, S. Hofbauer, I. Schaffner, B. Gasselhuber, A. Nicolussi, M. Soudi, K. F. Pirker, P. G. Furtmüller, C. Obinger, *Arch. Biochem. Biophys.* **2015**, *574*, 108 – 119.
[5] G. Battistuzzi, M. Bellei, C. A. Bortolotti, M. Sola, *Arch. Biochem. Biophys.* **2010**, *500*, 21 – 36.
[6] T. K. Kirk, R. L. Farrell, *Annu. Rev. Microbiol.* **1987**, *41*, 465 – 505.
[7] A. T. Martínez, F. J. Ruiz-Dueñas, M. J. Martínez, J. C. del Río, A. Gutiérrez, *Curr. Opin. Biotechnol.* **2009**, *20*, 348 – 357.
[8] A. J. Ragauskas, G. T. Beckham, M. J. Biddy, R. Chandra, F. Chen, M. F. Davis, B. H. Davison, R. A. Dixon, P. Gilna, M. Keller, P. Langan, A. K. Naskar, J. N. Saddler, T. J. Tschaplinski, G. A. Tuskan, C. E. Wyman, *Science* **2014**, *344*, 1246843.
[9] I. Ayuso-Fernández, A. T. Martínez, F. J. Ruiz-Dueñas, *Biotechnol. Biofuels* **2017**, *10*, 67.
[10] I. Ayuso-Fernández, F. J. Ruiz-Dueñas, A. T. Martínez, *Proc. Natl. Acad. Sci. USA* **2018**, *115*, 6428 – 6433.
[11] F. J. Ruiz-Dueñas, T. Lundell, D. Floudas, L. G. Nagy, J. M. Barrasa, D. S. Hibbett, A. T. Martínez, *Mycologia* **2013**, *105*, 1428 – 1444.
[12] D. Floudas, M. Binder, R. Riley, K. Barry, R. A. Blanchette, B. Henrissat, A. T. Martínez, R. Otillar, J. W. Spatafora, J. S. Yadav, A. Aerts, I. Benoit, A. Boyd, A. Carlson, A. Copeland, *Science* **2012**, *336*, 1715 – 1719.
[13] K. E. Hammel, D. Cullen, *Curr. Opin. Plant Biol.* **2008**, *11*, 349 – 355.
[14] D. Martinez, L. F. Larrondo, N. Putnam, M. D. Gelpke, K. Huang, J. Chapman, K. G. Helfenbein, P. Ramaiya, J. C. Detter, F. Larimer, P. M. Coutinho, B. Henrissat, R. Berka, D. Cullen, D. Rokhsar, *Nat. Biotechnol.* **2004**, *22*, 695 – 700.
[15] Z. H. Yang, *Mol. Biol. Evol.* **2007**, *24*, 1586 – 1591.
[16] T. L. Poulos, *Chem. Rev.* **2014**, *114*, 3919 – 3962.
[17] V. Sáez-Jiménez, M. C. Baratto, R. Pogni, J. Rencoret, A. Gutiérrez, J. I. Santos, A. T. Martínez, F. J. Ruiz-Dueñas, *J. Biol. Chem.* **2015**, *290*, 23201 – 23213.
[18] V. Sáez-Jiménez, J. Rencoret, M. A. Rodríguez-Carvajal, A. Gutiérrez, F. J. Ruiz-Dueñas, A. T. Martínez, *Biotechnol. Biofuels* **2016**, *9*, 198.
[19] F. J. Ruiz-Dueñas, A. T. Martínez, *Microb. Biotechnol.* **2009**, *2*, 164 – 177.
[20] G. Battistuzzi, M. Bellei, F. De Rienzo, M. Sola, *J. Biol. Inorg. Chem.* **2006**, *11*, 586 – 592.
[21] C. Ciaccio, A. Rosati, G. De Sanctis, S. Marini, R. Santucci, P. Ascenzi, K. G. Welinder, M. Coletta, *J. Biol. Chem.* **2003**, *278*, 18730 – 18737.
[22] C. D. Millis, D. Cai, M. T. Stankovich, M. Tien, *Biochemistry* **1989**, *28*, 8484 – 8489.
[23] M. Oyadomari, H. Shinohara, T. Johjima, H. Wariishi, H. Tanaka, *J. Mol. Catal. B-Enzym.* **2003**, *21*, 291 – 297.
[24] R. E. Whitwam, R. S. Koduri, M. Natan, M. Tien, *Biochemistry* **1999**, *38*, 9608 – 9616.
[25] R. Santucci, C. Bongiovanni, S. Marini, R. del Conte, M. Tien, L. Banci, M. Coletta, *Biochem. J.* **2000**, *349*, 85 – 90.
[26] M. Sørlie, L. C. Seefeldt, V. D. Parker, *Anal. Biochem.* **2000**, *287*, 118 – 125.
[27] J. Arnhold, P. G. Furtmüller, G. Regelsberger, C. Obinger, *Eur. J. Biochem.* **2001**, *268*, 5142 – 5148.
[28] P. G. Furtmüller, J. Arnhold, W. Jantschko, H. Pichler, C. Obinger, *Biochem. Biophys. Res. Commun.* **2003**, *301*, 551 – 557.
[29] P. G. Furtmüller, J. Arnhold, W. Jantschko, M. Zederbauer, C. Jakopitsch, C. Obinger, *J. Inorg. Biochem.* **2005**, *99*, 1220 – 1229.
[30] I. Efimov, N. D. Papadopoulou, K. J. McLean, S. K. Badyal, I. K. Macdonald, A. W. Munro, P. C. E. Moody, E. L. Raven, *Biochemistry* **2007**, *46*, 8017 – 8023.
[31] L. Castro, L. Crawford, A. Mutengwa, J. P. Goetze, M. Buehl, *Org. Biomol. Chem.* **2016**, *14*, 2385 – 2389.
[32] P. J. Kersten, B. Kalyanaraman, K. E. Hammel, B. Reinhammar, T. K. Kirk, *Biochem. J.* **1990**, *268*, 475 – 480.
[33] A. T. Martínez, *Enzyme Microb. Technol.* **2002**, *30*, 425 – 444.
[34] Z. S. Farhangrazi, M. E. Fossett, L. S. Powers, W. R. Ellis, *Biochemistry* **1995**, *34*, 2866 – 2871.
[35] C. W. Conroy, P. Tyma, P. H. Daum, J. E. Erman, *Biochimica et Biophysica Acta (BBA)—Protein Structure* **1978**, *537*, 62 – 69.
[36] X. S. Wang, S. Peter, R. Ullrich, M. Hofrichter, J. T. Groves, *Angew. Chem. Int. Ed.* **2013**, *52*, 9238 – 9241; *Angew. Chem.* **2013**, *125*, 9408 – 9411.
[37] I. Yamazaki in *Plant Peroxidases: Biochemistry and Physiology, IV International Symposium 1996; Proceedings* (Eds.: C. Obinger, U. Burner, R. Ebermann, C. Penel, H. Greppin), University of Geneva, Geneva, **1996**, pp. 34 – 41.
[38] L. Banci, I. Bertini, R. Pierattelli, M. Tien, A. J. Vila, *J. Am. Chem. Soc.* **1995**, *117*, 8659 – 8667.
[39] L. Banci, I. Bertini, E. A. Pease, M. Tien, P. Turano, *Biochemistry* **1992**, *31*, 10009 – 10017.
[40] L. Banci, I. Bertini, P. Turano, M. Tien, T. K. Kirk, *Proc. Natl. Acad. Sci. USA* **1991**, *88*, 6956 – 6960.
[41] L. Banci, I. Bertini, P. Turano, J. C. Ferrer, A. G. Mauk, *Inorg. Chem.* **1991**, *30*, 4510 – 4516.
[42] L. Banci, S. Camarero, A. T. Martínez, M. J. Martínez, M. Pérez-Boada, R. Pierattelli, F. J. Ruiz-Dueñas, *J. Biol. Inorg. Chem.* **2003**, *8*, 751 – 760.
[43] I. Bertini, P. Turano, A. J. Vila, *Chem. Rev.* **1993**, *93*, 2833 – 2932.
[44] G. N. La Mar, *IUBMB Life* **2007**, *59*, 513 – 527.
[45] G. N. La Mar, J. S. Deropp, V. P. Chacko, J. D. Satterlee, J. E. Erman, *Biochim. Biophys. Acta* **1982**, *708*, 317 – 325.
[46] J. D. Satterlee, J. E. Erman, *Biochemistry* **1991**, *30*, 4398 – 4405.
[47] T. Inubushi, E. D. Becker, *J. Magn. Reson. (1969-1992)* **1983**, *51*, 128 – 133.
[48] S. Kumar, G. Stecher, M. Li, C. Knyaz, K. Tamura, *Mol. Biol. Evol.* **2018**, *35*, 1547 – 1549.
[49] A. Stamatakis, P. Hoover, J. Rougemont, *Syst. Biol.* **2008**, *57*, 758 – 771.

Manuscript received: November 14, 2018
Accepted manuscript online: December 19, 2018
Version of record online: January 25, 2019

